Article

Improved Metaheuristic-Driven Energy-Aware Cluster-Based Routing Scheme for IoT-Assisted Wireless Sensor Networks

Kuruva Lakshmanna [1], Neelakandan Subramani [2,*], Youseef Alotaibi [3], Saleh Alghamdi [4], Osamah Ibrahim Khalafand [5] and Ashok Kumar Nanda [6]

1   Department of Information Technology, Vellore Institute of Technology, Vellore 632014, India; lakshman.kuruva@vit.ac.in
2   Department of Computer Science and Engineering, R.M.K Engineering College, Chennai 601206, India
3   Department of Computer Science, College of Computer and Information Systems, Umm Al-Qura University, Makkah 21955, Saudi Arabia; yaotaibi@uqu.edu.sa
4   Department of Information Technology, College of Computers and Information Technology, Taif University, Taif 21944, Saudi Arabia; s.algamedi@tu.edu.sa
5   Department of Computer Engineering, Al-Nahrain Nano Renewable Energy Research Center, Al-Nahrain University, Baghdad 10071, Iraq; usama81818@nahrainuniv.edu.iq
6   Department of Computer Science and Engineering, B V Raju Institute of Technology, Narsapur 502313, India; ashokkumar.nanda@bvrit.ac.in
*   Correspondence: snksnk17@gmail.com

Abstract: The Internet of Things (IoT) is a network of numerous devices that are consistent with one another via the internet. Wireless sensor networks (WSN) play an integral part in the IoT, which helps to produce seamless data that highly influence the network's lifetime. Despite the significant applications of the IoT, several challenging issues such as security, energy, load balancing, and storage exist. Energy efficiency is considered to be a vital part of the design of IoT-assisted WSN; this is accomplished by clustering and multi-hop routing techniques. In view of this, we introduce an improved metaheuristic-driven energy-aware cluster-based routing (IMD-EACBR) scheme for IoT-assisted WSN. The proposed IMD-EACBR model intends to achieve maximum energy utilization and lifetime in the network. In order to attain this, the IMD-EACBR model primarily designs an improved Archimedes optimization algorithm-based clustering (IAOAC) technique for cluster head (CH) election and cluster organization. In addition, the IAOAC algorithm computes a suitability purpose that connects multiple structures specifically for energy efficiency, detachment, node degree, and inter-cluster distance. Moreover, teaching–learning-based optimization (TLBO) algorithm-based multi-hop routing (TLBO-MHR) technique is applied for optimum selection of routes to destinations. Furthermore, the TLBO-MHR method originates a suitability purpose using energy and distance metrics. The performance of the IMD-EACBR model has been examined in several aspects. Simulation outcomes demonstrated enhancements of the IMD-EACBR model over recent state-of-the-art approaches. IMD-EACBR is a model that has been proposed for the transmission of emergency data, and the TLBO-MHR technique is one that is based on the requirements for hop count and distance. In the end, the proposed network is subjected to rigorous testing using NS-3.26's full simulation capabilities. The results of the simulation reveal improvements in performance in terms of the proportion of dead nodes, the lifetime of the network, the amount of energy consumed, the packet delivery ratio (PDR), and the latency.

Keywords: Internet of Things; WSN; clustering; route selection; metaheuristics; fitness function; network lifetime; energy efficiency

1. Introduction

In recent times, the Internet of Things (IoT) and mobile edge computing (MEC) are becoming familiar components in fulfilling forthcoming technical necessities. The technological expansions mainly focus on the demand for information transfer, minimizing load

on the network, and throughput [1]. Handling minimum postponement, data memory storage, and being able to function in crucial application zones are the requirements for networks in smart grids, smart cities, reliable platforms, and in transportation [2]. The growing amount of data could be dealt with using MEC gadgets that have a specific groundwork for obtaining network analytics, and network optimization by using IoT. With rapidly increasing numbers of IoT gadgets, the creation of self-governing networks for IoT gadgets has received increasing attention by scientists [3]. In the concept of network executives, the chief goal is to create a power-proficient multi-hop network that can connect source-to-destination nodes via mobile phone relay nodes (RNs) through the use of power restraints [4]. Thus, the network topologies are termed respectively in order to wirelessly connect between RNs, which are IoT gadgets.

As a result of recent progression in microelectromechanical system (MEMS) technologies and wireless networks, wireless sensor networks (WSNs) have garnered significant attention by different applications such as military, healthcare, disaster management, industrial automation, etc. [5]. Wireless sensor networks (WSN) are an integral part of the IoT. Therefore, WSN applications have found associations in society, the computing world, and the physical world. In common terms, WSNs comprise a large number of tiny sensors dispersed over a vast area, accompanied by base stations (BS) that assemble information from these sensor nodes. All sensor nodes (SN) have restricted power supplies, and have the abilities to process data, sense, and transmit [6]. Hierarchical-based (or cluster-based) routing is a familiar method with some specific benefits that relate to scalability and efficiency in communications. The concepts of hierarchical routing have been implemented in order to attain power efficiency in WSNs [7]. In contrast, lower power nodes are used only for sensor related work in areas that are nearer to the target. Thus, making clusters and allocating specific jobs to cluster heads (CHs) can importantly donate to the scalability of the system, its lifespan, and its power efficiency. Scalability is a critical aspect in WSNs that has not been well established in many of the protocols as a result of the initial assumptions made. For example, cluster-based protocol generally considers one sink with cluster heads inside the coverage of the sink [8]. Under those considerations, WSNs lack scalability, and result in communications that are excessive in terms of their power requirements. Hence, slightly raising the total quantity of device nodes or the width of the network will lead to overloading that develops exponentially, and a hindrance that contains only a single sink; these can strangle the network. Hierarchical routing is an effective way to diminish power utilisation inside the cluster and perform information accumulation. In addition to this, this approach permits merging tasks to decrease the number of transferred packets to the sink [9]. All perceptions of the nodes, from hardware devices to their accomplished processes, will aid in distributing the power load [10]. Thankfully, hierarchical routing has several roles to assist us in distinguishing potential stages in protocol processes; the availability of two operation modes in the sensor nodes can estimate comparatively higher energy expenses. However, various transmission modes, namely cluster heads and normal sensors, may become advantageous if executed in every layer.

This project emphasises the use of a better metaheuristic-driven energy-aware cluster-based routing (IMD-EACBR) scheme for IoT-assisted WSN. The proposed IMD-EACBR model initially derives an improved Archimedes optimization algorithm-based clustering (IAOAC) technique. In addition, the IAOAC algorithm computes a fitness function that involves multiple parameters, namely energy efficiency, distance, node degree, and inter-cluster distance. Moreover, teaching–learning-based optimisation (TLBO) algorithm-based multi-hop routing (TLBO-MHR) technique was executed for the optimum selection of routes to destinations. The design of IAOAC and TLBO-MHR techniques with multiple input parameters depicts the innovation of the research. The presentation of the IMD-EACBR model has been examined in several aspects.

In this paper, we propose the IMD-EACBR, a new routing strategy for WSNs that uses a mix of a clustering methodology and a TLBO-MHR technique to extend network lifetime. The goal of the proposal is to find the best route from the source to the destination

by prioritising the maximisation of remaining battery power, the minimisation of energy consumed in a multi-hop path, and the greatest equity across sensor nodes. The simulation results show that this protocol not only balances the overall network's energy usage, it also delays node death time and provides more dependable data delivery.

The core donations and innovations of this investigation are as follows:

i.　Multi-hop directing methods are thought to be energy-effective explanations for wireless device systems, which address a problem known as gathering. On the other hand, the cluster-based directing techniques used in conventional wireless networks might not be appropriate to WSN due to factors such as the presence of an underwater present, a limited bandwidth, a high water compression, a prolonged broadcast latency, and an increased error prospect.

ii.　In order to tackle these challenges and achieve energy efficiency in WSNs, the primary focus of this research is on the making of a metaheuristic-based gathering along with a directing procedure for WSNs. This protocol is given the name IMD-EACBR.

iii.　The IMD-EACBR technique selects the most advantageous CHs and the most direct paths to the BS. IMD-EACBR is a method that employs the teaching–learning-based optimization (TLBO) optimizer-based gathering in order to select the most suitable CHs and construct appropriate collections.

iv.　In order to demonstrate the manner in which the IMD-EACBR technique enhances performance, a number of simulations are carried out, and the results are analysed in a variety of different ways.

The remaining portion of the paper is divided into five sections that are descriptive in nature. In the second section, an assessment of preceding efforts that have been made in the same context is presented, in order to classify the practical gaps. In Section 3, the plan is broken down into its individual IAOAC phases for clarity. The study is brought to a close with a discussion of the potential directions of IAOAC in the years to come. Section 4 provides an in-depth analysis of the presentation, in order to validate the superiority and effectiveness of IAOAC. Section 5 presents the conclusions.

2. Literature Review

Kavitha, A. et al. [11] proposed a cluster-based routing with simulated annealing and genetic algorithm-based hybrid (SAGA-H) method. The presented technique was simulated and explained by utilizing MATLAB. Furthermore, the observed results were compared to a contemporary genetic algorithm (GA)-based method regarding average residual energy, network lifespan, and the number of packets transmitted between the BS and sink.

Subbulakshmi, P. et al. [12] introduced a multiple-objective founded gathering and Sailfish Optimizer (SFO)-directed protocol to augment energy efficiency in WSNs. The CH is chosen based on fitness criteria that are expressed from multiple objectives. It assists in reducing the number of dead sensors and minimises energy utilization. Following CH selection, SFO is utilised to select an optimum route to a sink node for transmitting information. The presented method was analysed, and results were compared to current techniques.

Gowda, C.S. et al. [13] proposed a novel hybrid neural network (NN)-based energy-effective routing method by using routing protocol (RP). Firstly, the sensors are clustered by the mean shift clustering method. Next, the bald eagle search approach chooses the CH to clustered node. Subsequently, RP is chosen rather than visiting each CH. Then, the RP is selected according to the weight assessment among hop distances and the amount of transferred data packets. At last, a hybrid NN using group teaching algorithm was presented for determining the optimal route.

Vaiyapuri et al. [14] presented an IoT-assisted cluster-based routing (CBR) method for information-centric WSNs (ICWSN), named CBR-ICWSN. The proposed method undergoes a black widow optimization (BWO)-founded gathering approach for efficiently choosing an optimal set of CHs. Furthermore, the CBR-ICWSN approach comprises an oppositional ABC (OABC)-based routing method for better election of routes.

Shafiq et al. [15] proposed a robust cluster-based routing protocol (RCBRP) to recognize the routing path by which minimal energy is expended, in order to enhance network lifespan. The presented method was composed of transmission and explored ow methods. Then, is the study presented two approaches: (i) distance and energy consumption assessment method, and (ii) routing and energy-effective bunch technique.

Zheng et al. [16] presented a stability-aware cluster-based routing (SACR) approach for CRSN. In terms of cluster formation, the study presented range subtleties and energy utilisation in the clustering method.

Awan et al. [17] proposed a metaheuristic artificial intelligence approach based on the social behavior of grey wolves, in order to minimise the energy utilization of WSNs from the livestock industry. The energy level, grid size, transmission range, and direction were the major parameters utilised for measuring the algorithm's performance. The following Table 1 describes the existing approach methodologies.

Table 1. Summary of existing approaches.

Reference No.	Published Year	Approach	Advantages	Disadvantages
[11]	2020	Simulated annealing and genetic algorithm-based hybrid (SAGA-H)	Self-organization	High communication cost
[12]	2018	Clustering and Sailfish Optimizer (SFO)	Low communication cost	High latency
[13]	2021	Novel hybrid NN based energy-effective routing	Load complementary	High latency, low scalability
[14]	2021	Cluster based routing (CBR)	Fast convergence, low overhead	Low coverage
[15]	2022	Robust cluster-based routing protocol (RCBRP)	Minimum overhead, low latency	Only uniform node distribution
[16]	2021	Stability-aware cluster-based routing (SACR)	Support node heterogeneity	Low scalability
[17]	2022	Metaheuristic artificial intelligence approach based on social behavior of grey wolves	Prolongs network lifetime	Needs parameter adjustments

O. J. Pandey et al. [18] presented LPWANs, a multi-hop data directing approach. Since the multi-hop data program encounters a number of obstacles, including augmented data dormancy, increased meddling, and decreased data quantity (i.e., inefficient utilisation of bandwidth), we suggest a reinforcement learning strategy to handle these obstacles. The suggested technique updates the network's Q-matrix at periodic time intervals and picks relay devices to exploit the increasing prize rate between designated device–gateway pairings. Furthermore, we present a novel data routing mechanism that optimises the energy rate of the cables. This strategy results in unchanging energy use and accelerated data transport. On a WSN testbed, simulations and actual node deployments are used to conduct experiments [19]. In order to prevent sensor nodes from behaving selfishly in future operations, a consequence instrument is developed to compel device nodes to embrace cooperative methods. The simulation findings demonstrate that game theory may efficiently reduce the sensor network's energy consumption and enhance the amount of data transmission, thus achieving the goal of extending the network's lifetime [20].

3. Materials and Methods

In this article, a new IMD-EACBR method has been designed to maximise energy efficiency and lifetimes of WSNs. At the primary level, the IoT nodes in the network are randomly placed and communicate with one another for the information collection process. Then, the presented IMD-EACBR technique primarily selects CHs and organizes clusters using the IAOAC technique. This is followed by the optimal selection of routes using the TLBO-MHR technique. Once the optimal routes are identified, the CHs use optimal routes for transmitting data to a BS. Figure 1 demonstrates the general procedure of the proposed IMD-EACBR method.
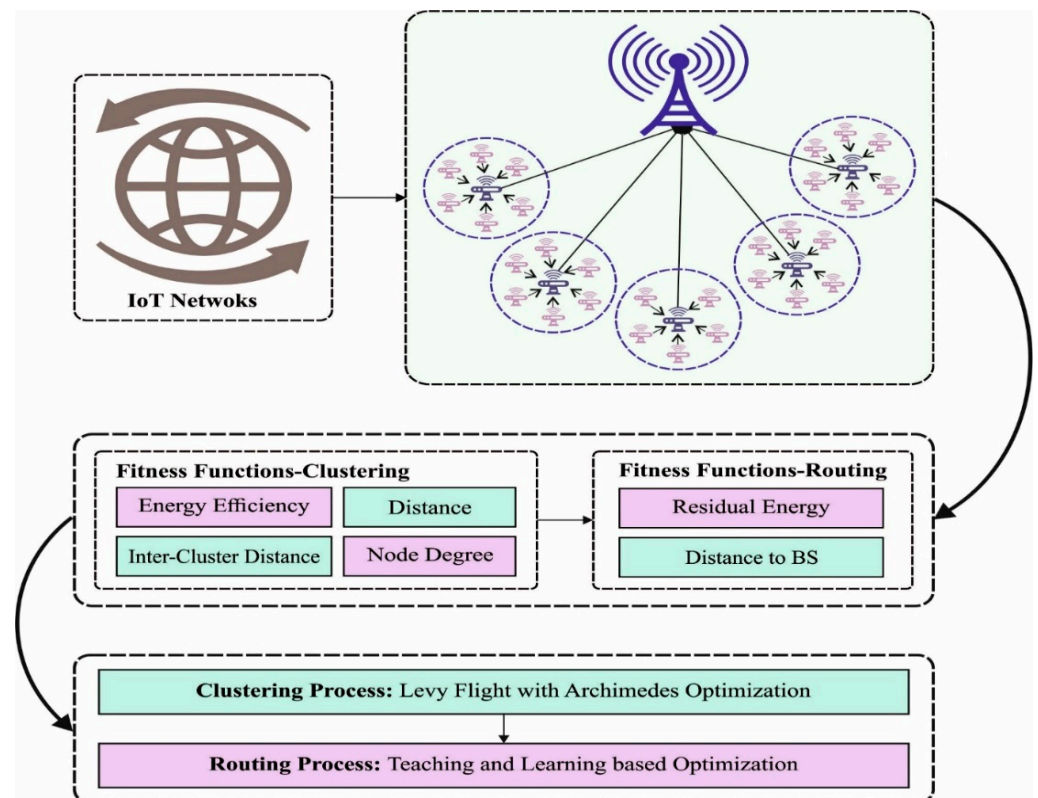
Figure 1. Overall process of the IMD-EACBR technique.

Srilakshmi, U. et al. [21] introduced AOA, inspired by the work of Archimedes, that can be determined from rules of physics. The presented method focused on the object that was completely or partially immersed in the fluid. The initialisation procedure of each object can be implemented by Equation (1):

$$0_i = l_i + rand \times (u_i - l_i), i = 1, 2, \ldots, N \tag{1}$$

where l_i and u_i indicate the lower and upper bounds of ith object, respectively, and N denotes the number of objects. Rand are numbers that are produced at random and are spread out evenly across the range [0, 1]; rand can refer to a scale factor in the range [0, 1]. The density and volume of all the objects are initialised by the following equation:

$$den_i = rand, vol_i = rand \tag{2}$$

3.1. Algorithmic Process of IAOA Technique

Here, rand denotes a vector of D-dimensional value within [0, 1]. The acceleration of an object is evaluated by the following equation:

$$acc_i = lb_i + rand \times (ub_i - lb_i) \tag{3}$$

The suitability purpose is evaluated, and the object with the optimal fitness value is allocated by x^{best}, den^{best}, vol^{best}, and acc^{best}.

The updating procedure for the ith object's volume and density can be implemented by the following equations:

$$den_i^{t+1} = den_i^t + rand \times \left(den^{best} - den_i^t \right) \tag{4}$$

$$vol_i^{t+1} = vol_i^t + rand \times \left(vol^{best} - vol_i^t \right) \tag{5}$$

where t denotes the present iteration and rand indicates an arbitrary value. It can be shown in the following equation:

$$TF = exp\left(\frac{t - t_{max}}{t_{max}}\right) \tag{6}$$

The transfer operator (TF) aids the alteration of AOA exploration, from the exploration stage to the misuse phase, as shown in Equation (6). The TF rate steadily rises over the period pending the unity value 1, where TF is the transfer operator capable of transferring the operator search procedure from the examination to the mistreatment stage. Then, t_{max} denotes the maximum quantity of repetitions. Next, the values of TF are increasingly improved through iteration. The density decreasing factor assists the AOA to transfer from the global to a local searching space, and is expressed in the following equation:

$$d^{t+1} = TF - \left(\frac{t}{t_{max}}\right) \tag{7}$$

The values of d^{t+1} decrease with time; furthermore, suitable allocations of parameters assist in achieving a balance between the exploitation and exploration stages. While t is the number of repetitions, t max is the supreme quantity of repetitions. The exploration stage refers to collisions among the substances; this stage is measured once the transmission operative is 0.5. The hastening of the ith object at iteration $t + 1$ can be upgraded by choosing an arbitrary material (mr) in the following equation [22]:

$$acc_i^{t+1} = \frac{den_{mr} + vol_{mr} \times acc_{mr}}{den_i^{t+1} \times vol_i^{t+1}} \tag{8}$$

where n_{mr}, vol_{mr}, and acc_{mr} indicate the thickness, capacity, and quickening of random material (mr), respectively. The acceleration of the ith object in the exploitation stage is evaluated with the following equation:

$$acc_i^{t+1} = \frac{den_{best} + vol_{best} \times acc_{best}}{den_i^{t+1} \times vol_i^{t+1}} \tag{9}$$

In Equation (9), n_{best}, vol_{best}, and acc_{best} indicate the object's thickness, capacity, and hastening, respectively. It can be significant to standardize the acceleration of all the particles; this defines the step percentage by which all the particles would change. It can be formulated with the following equation:

$$acc_{i-norm}^{t+1} = u \times \left(\frac{acc_i^{t+1} - \min(acc)}{\max(acc) - \min(acc)}\right) + l \tag{10}$$

where l and u denote the normalization range, allocated as 0.1 and 0.9, respectively. Once the object is farther from the international optimal, the value of hastening would be higher; in such cases, the examination stage is presented, otherwise mistreatment stage is conducted.

The location of the ith element is upgraded in the examination stage as follows:

$$\chi_i^{t+1} = \chi_i^t + C_1 \times rand \times acc_{i-norm}^{t+1} \times d \times \left(\chi_{rand} - \chi_i^t\right) \tag{11}$$

At the same time, the updating procedure for particle position in the exploitation stage is given in the following equation:

$$\chi_i^{t+1} = \chi_i^t + F \times C_2 \times rand \times acc_{i-norm}^{t+1} \times d \times \left(T \times \chi_{best} - \chi_i^t\right) \tag{12}$$

where C_1 and C_2 denote constants (C) determined by the user, T indicates a variable which is based on the transfer operator $(T = C_3 \times TF)$, C_3 indicates a continuous rate, χ_{best}

represents the location of the optimal subdivision, and *F* indicates the flag applied to alter the element movement path.

The IAOA is derived using Levy flight (LF) approach in the classical AOA [23–27]. It is an arbitrary walk where the steps are determined with respect to the step length that has a detailed probability distribution. An arbitrary step length is drawn in a Levy distribution (LD) that is determined with following formula [28]:

$$L(s) \sim |s|^{-1-\beta} \tag{13}$$

where $\beta(0 < \beta \le 2)$ refers the catalog, and *s* is the stage measurement. The Mantegna algorithm for symmetric Levy stable distribution is utilised to create arbitrary step sizes. In Mantegna's procedure, the step measurement *s* is measured as follows:

$$s = \frac{u}{|v|^{\frac{1}{\beta}}} \tag{14}$$

where *u* and *v* are drawn from a normal distribution, as follows:

$$u \sim N\left(0, \sigma_u^2\right), v \sim N\left(0, \sigma_v^2\right) \tag{15}$$

This distribution follows the expected LD for $|s| \ge |s_0|$, whereas s_0 refers to the minimum step length. During the presented approach, the step sizes are created by utilising an LD to exploit the search region, and are computed as follows:

$$step_{size(t)} = 0.001 \times s(t) \times SLC \tag{16}$$

where *t* refers to the iteration counter for the local search approach, $s(t)$ has been computed utilising an LD, and *SLC* denotes the social learning component of the global searching technique.

3.2. Process Involved in IAOAC Technique

Once the nodes are deployed in the region of interest, the IAOAC technique is executed. The IAOAC method was developed with the presence of four suitability features, including the energy competence of IoT device nodes, the compactness of cluster nodes, the regular detachment of IoT devices for CHs contained by their sensing series, and the distances of CHs to sinks. The data on fitness parameters are shown in Equation (17).

Energy competence: The CHs execute many events such as sensing, gathering, aggregation, data broadcast, etc.; thus, CHs intake more energy than other nodes. Hence, they can be vital to determine a fitness function (FF) that shares the load among all of the IoT devices from the system. The suitability limit for effective deployment of system energy is determined as follows:

$$R_e = e(n_i)$$
$$Avg_e = \frac{1}{n} \sum_{i=0}^{n} e(n_i)$$
$$f_1 = CH_{opt} * \frac{R_e}{Avg_e} = \frac{CH_{opt}*e(n_i)}{\frac{1}{n}\Sigma_{i=0}^{n}e(n_i)} \forall CH_{opt} = 5\% \ of \ n, \ e(n_i)$$
$$= 0.5J \ or \ 1.25J \ or \ 1.75J \tag{17}$$

where R_e, Avg_e, and n_i refer to the node RE, network average energy, and total amount of IoT device nodes from the system, respectively. CH_{opt} signifies the optimum percentage of CHs.

The number of nodes in a cluster is an important parameter to consider when trying to improve the energy efficiency of networks, since it affects the cost of intra-cluster

transmissions. The cluster cost function was defined using the supplied function, which meant that the network energy deployment was of a higher quality than before:

$$f_2 = max\ (n(CH_1), n(CH_2), n(CH_3)n(CH_j)),\ \forall n = 2\ to\ 95,\ j = 1\ to\ 15 \qquad (18)$$

where $n(CH_j)$ refers to the number of IoT devices from the range of the jth CH (CH_j). The value of objective function f_2 is higher than any choice of CH, and is utilised in decreasing the energy reduction.

The regular detachment of IoT devices to the CH within its detection range occurs in intra-cluster transmission, and when IoT devices transmit data to CH. If the CH is away from CM, then IoT devices diminish their energy consumption once the CH is nearer to the member IoT device node; afterward, it deploys minimal energy.

$$f_3 = \frac{1}{n_{s\tau}} \sum_{i=0}^{n_{sr}} dist(CH, i)\ \forall dist(CH, i) = 1\ to\ 35\ m, n_{sr} = 1\ to\ 100 \qquad (19)$$

where n_{sr} and $dist(CH, i)$ signify the number of IoT devices from a sensing series and the Euclidean distance in node and CH from the perception sequence of individual clusters, respectively. Therefore, the rate of f_3 is minimal but the diminishing intra-cluster transmits power.

Detachment from CH to Base Station(BS): When using CH selection (CHS), however, the distances among the CHs and BSs are quite important. The reason for this is because the supplied function forecasts that if the CHs are located a significant distance from the sink, they will use energy at a rapid rate:

$$f_4 = \frac{1}{CH} \sum_{i=0}^{CH} dist(BS, CH_i)\ \forall dist(BS, CH_i) = 1\ to\ 70m,\ CH = 1\ to\ 15 \qquad (20)$$

where $dist(BS, CH_i)$ implies the Euclidean distance between the BS and the ith CH (CH_i). Minimising the f_4 impartial purpose states that the CHs are not far away from the BS.

When the f_1, f_2, f_3, and f_4 purpose strictures are measured, the impartial purpose is called FF, which is represented as follows:

$$FF = Maximize\ Fitness = \alpha * f_1 + \beta * f_2 + \gamma * \frac{1}{f_3} + \delta * \frac{1}{f_4} \qquad (21)$$

where α, β, γ, and δ signify the weight coefficients to f_1, f_2, f_3, and f_4 FF parameters, respectively. The range of weight coefficients is varied between *zero* and one.

3.3. Design of TLBO-MHR Technique

When the CHs are chosen and clusters are optimally generated, the TLBO-MHR algorithm is applied to generate optimal routes in the IoT-assisted WSN. TLBO is a population-based technique simulated by the procedure of teacher as well as learner [29–36]. Differing from other heuristic techniques, TLBO requires fewer approaches to certain parameters, which is an essential reason for choosing TLBO technique to optimize problems. Other heuristic approaches are heavily dependent on the parameter chosen; that is a significant limitation, as its efficiency is heavily dependent upon parameter tuning. A minor change from some parameters can affect the efficacy of the entire technique.

TLBO begins by creating an arbitrary primary population, and then upgrades that population from all its iterations [37–43]. The rows match to learner, whereas columns relate to subjects. All the subjects of the learner signify the grade of application, while the entire quantity of topics of a beginner assemble to periods on which preparation is executed. The purpose of all the learners is to exploit their skills in all the subjects. The procedure of TLBO was separated into two stages: teacher and learner phases. During the teacher stage, the mean of learners from all the subjects is computed. The fitness of

all learners is measured, and the optimum learner is then chosen as a teacher $\left(X_{old}^g \right)$. A novel vector is furthered to represent a population that is created in the existing mean and optimum mean vector, as follows:

$$X_{new(i)}^g = X_{(i)}^g + r \times \left(X_{main}^g - T_f M^g \right) \tag{22}$$

where r represents the arbitrarily created number between zero and one. T_f signifies the instructor factor and its rate is either 1 or 2.

The rate of T_f is arbitrarily chosen as follows:

$$T_f = round[1 + r_1] \tag{23}$$

where r_1 refers to the arbitrary quantity with a rate between zero and one. T_f is not an input parameter and is arbitrarily obvious by the technique utilised in Equation (12). The value of T_f is chosen as either 1 or 2, depending on rounding up conditions. If $X_{new(i)}^g$ is superior in fitness to $X_{(i)}^g$, then $X_{(i)}^g$ is exchanged by the higher learner $X_{new(i)}^g$. Random variables rand1 and rand2 are accidental numbers with a uniform delivery in the interval [0, 1] and are a scale factor in the interval [0, 1].

During the learner stage, the learner interrelates with everyone and enhances his or her data through mutual communication [44–48]. All the learners relate with other learners for the sake of data sharing. From among all learners $X_{(i)}^g$, another learner $X_{(r)}^g$ is arbitrarily chosen ($i \neq r$) and the population is upgraded as follows:

$$X_{new(i)}^g = \begin{cases} X_{(i)}^g + rand \times \left(X_{(i)}^g - X_{(r)}^g \right) & if \ X_{(i)}^g \leq X_{(r)}^g \\ X_{(i)}^g + rand \times \left(X_{(r)}^g - X_{(i)}^g \right) & otherwise \end{cases} \tag{24}$$

The algorithm endures until the condition is met. Algorithm 1 provides the entire mechanism of TLBO. Figure 2 shows the flow chart of the TLBO method.

Algorithm 1: TLBO Algorithm

Input: Populace size (pop-size), quantity of topics, end condition
Initialisation: Create primary people
while terminating condition is not met do
    Teacher phase
    Choose the optimum separate as a teacher $x_{Teacher}^g$ in people
    Compute the mean charge (x_m) of all the subjects
    for $i = 1$ to popsize do
        $T_F = round(1 + rand(0,1))$
        $x_i^{new} = x_i^{old} + rand_i(x_{Teacher}^g - T_F \times x_m)$
        Compute fitness of novel individual $f(x_i^{new})$
        if $f(x_i^{new}) < f(x_i^{old})$ then
            $x_i^{old} = x_i^{new}$
        end
    end
  Learner phase
    for $i = 1$ to popsize do
    Choose an arbitrary individual x_r so as $r \neq i$
    if $f(x_i) < f(x_r)$ then
        $x_i^{new} = x_i^{old} + rand_i(x_r - x_i)$
    else
        $x_i^{new} = x_i^{old} + rand_i(x_i - x_r)$
    end
    end
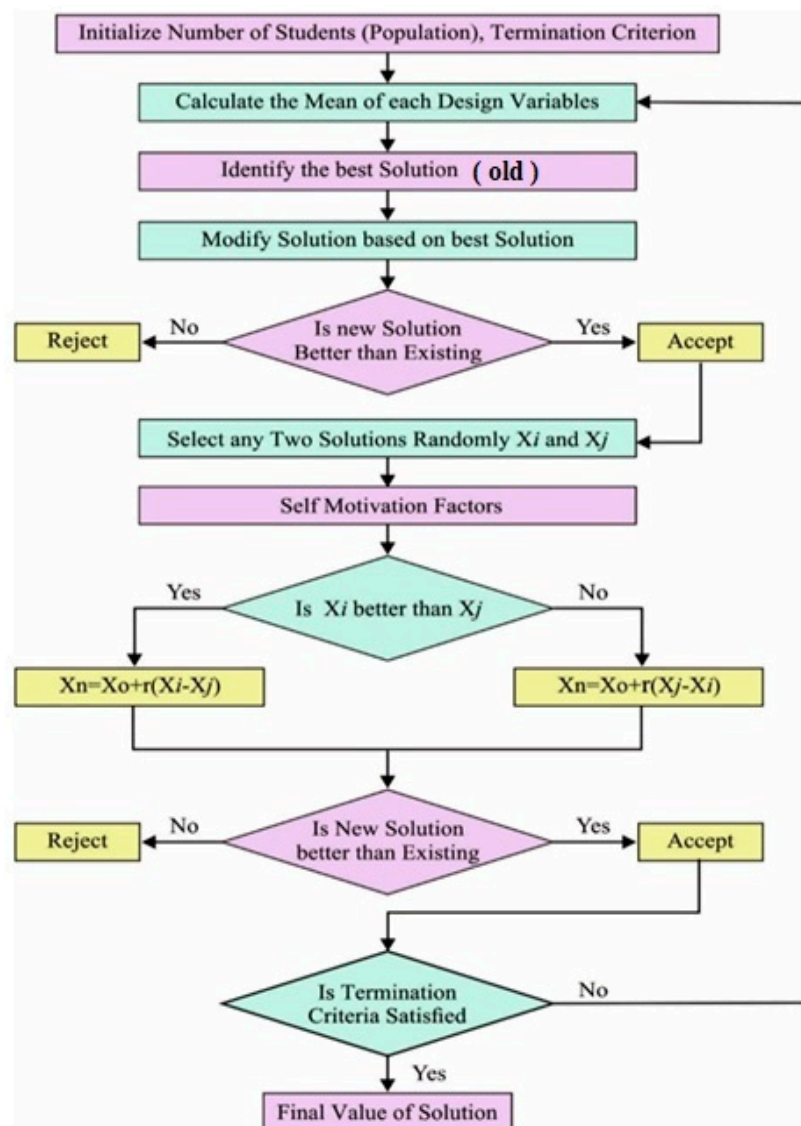 end
  end
Return Best

Figure 2. Flowchart of the TLBO technique.

During instruction, to define the best group of routes, the TLBO-MHR procedure is applied in order to determine the subsequent hop to BS. This can be shown in the following:

$$f(x) = \left\{ i, \text{ For Which} \left| \left(\frac{i}{k} - X_{i_{f}j} \right) \right| \text{is Minimum, } \forall \, i \quad and \quad 1 \leq i \leq k \right\} \tag{25}$$

The procedure aims to define the best group of routes in CHs to the BS through an FF that contains two variables, such as distance and energy [49–53]. Initially, the RE of the next-hop node is described, and the node with maximum energy serves as the RN. Hence, the node with superior RE becomes the next-hop node. This is given in the following:

$$f1 = E_{CH} \tag{26}$$

Furthermore, the Euclidean distance is executed for defining the distance in a CH to BS. Using minimum distance, the energy consumption is kept significantly low [38,54–57]. When the distance is increased, additional energy is expended. Thus, the node with lowest distance is chosen as an RN, as follows:

$$f2 = \frac{1}{\sum_{i=1}^{m} dist(CH_i, \ NH) + dist(NH, \ BS)} \tag{27}$$

The above-mentioned sub-objective is studied relative to FF, where α_1 and α_2 denote the weights assigned to each sub-objective.

$$Fitness = \alpha_1(f1) + \alpha_2(f2), \;\; where \;\; \alpha_1 + \alpha_2 = 1 \,; \;\; \alpha_i \in (0, 1) \tag{28}$$

4. Experimental Validation

In this section, a complete proportional training of the IMD-EACBR model compared to other current models is carried out. A route damage prototype founded on a cluster is created using both the CI and FI representations. Large-scale features such as PLEs and shadow factors in LOS and NLOS instances are designed and associated with those of the NYU prototype in the same setting.

Table 2 and Figure 3 report a brief network lifetime (NLT) examination of the IMD-EACBR model compared to other approaches. The results indicate that the IMD-EACBR model accomplished a maximum NLT under all SNs [58–67]. For instance, with 100 SNs, the IMD-EACBR model attained an maximum NLT of 1719 rounds, whereas the sunflower optimisation (SFO), gray wolf optimisation (GWO), genetic algorithm (GA), ant line optimisation (ALO), and particle swarm optimisation (PSO) models obtained reduced NLTs of 1593, 1448, 1415, 1349, and 1300 rounds, respectively. Furthermore, with 500 SNs, the IMD-EACBR model reached a superior NLT of 3500 rounds, whereas the SFO, GWO, GA, ALO, and PSO models resulted in lower NLTs of 3501, 3395, 3263, 2966, and 2684 rounds, respectively.

Table 2. NLT analysis of the IMD-EACBR technique compared to other approaches under various densities of SNs.

|	Network Lifetime (Rounds)					
Density of Sensor Nodes	IMD-EACBR	SFO Alg.	GWO Alg.	Genetic Alg.	ALO Alg.	PSO Alg.
100	1719	1593	1448	1415	1349	1300
150	1950	1739	1653	1554	1442	1380
200	2135	1956	1791	1706	1547	1456
250	2438	2174	2082	1818	1692	1538
300	2590	2392	2286	2009	1871	1687
350	2847	2656	2570	2359	2062	1984
400	3092	2887	2808	2643	2379	2165
450	3283	3098	3045	2953	2630	2354
500	3500	3501	3395	3263	2966	2684
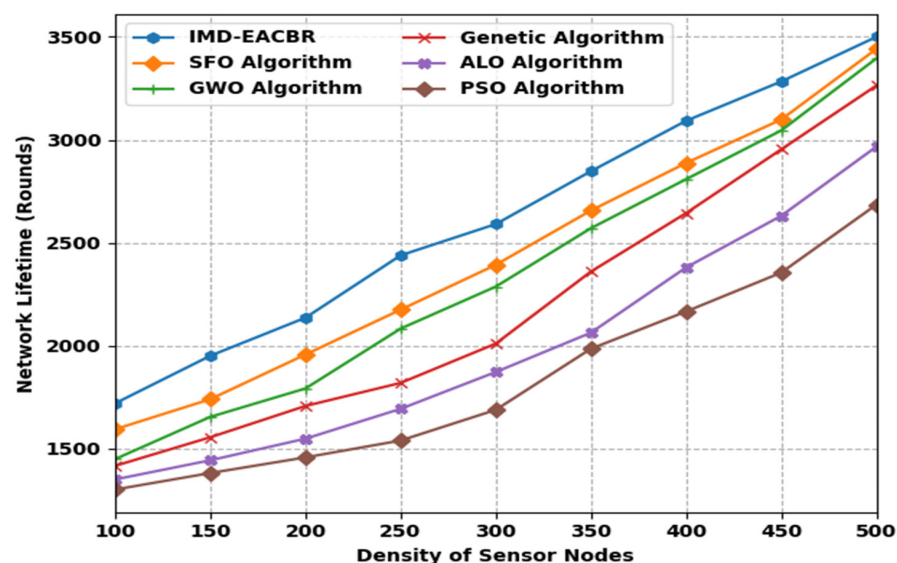
Figure 3. NLT analysis of the IMD-EACBR technique under various densities of SNs.

Table 3 and Figure 4 demonstrate the number of alive sensor nodes (NOASN) analysis of the IMD-EACBR method and of other models. The results indicate that the IMD-EACBR model accomplished maximum NOASN under all rounds. For instance, with 2000 rounds, the IMD-EACBR approach attained an increased NOASN of 468, whereas the SFO, GWO, GA, ALO, and PSO models obtained reduced NOASNs of 444, 404, 373, 295, and 278, respectively. Simultaneously, with 3250 rounds, the IMD-EACBR prototype achieved the highest NOASN of 315, whereas the SFO, GWO, GA, ALO, and PSO approaches achieved occasional to few NOASNs of 176, 52, 10, 5, and 2, respectively.

Table 3. NOASN study of the IMD-EACBR procedure compared to other methods for different numbers of rounds.

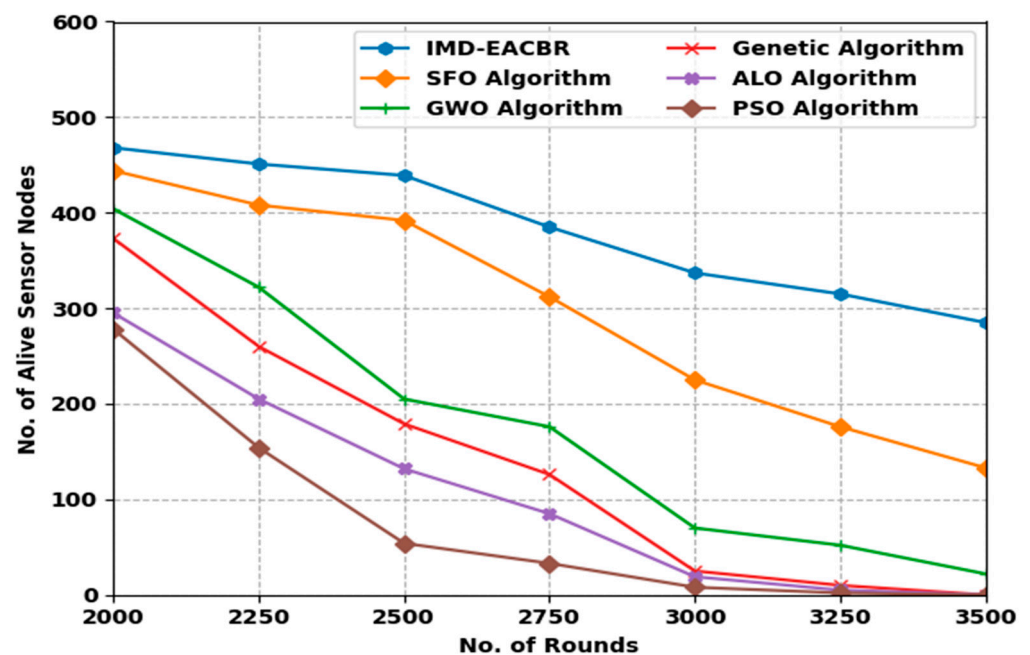| No. of Alive Sensor Nodes						
No. of Rounds	IMD-EACBR	SFO Alg.	GWO Alg.	Genetic Alg.	ALO Alg.	PSO Alg.
2000	468	444	404	373	295	278
2250	451	408	322	260	205	154
2500	439	392	205	179	132	54
2750	385	312	176	126	85	33
3000	337	225	70	25	19	8
3250	315	176	52	10	5	2
3500	285	133	22	0	0	0

Figure 4. NOASN analysis of the IMD-EACBR technique under varying numbers of rounds.

A comprehensive proportional examination of the IMD-EACBR model compared to current models in terms of numbers of dead sensor nodes (NODSN) is shown in Table 4 and Figure 5. The outcomes exhibit that the IMD-EACBR approach resulted in effective outcomes with negligible values of NODSNs [18,19,68–70]. For example, with 2000 rounds, the IMD-EACBR model achieved a decreased NODSN of 215 nodes, whereas the SFO, GWO, GA, ALO, and PSO models resulted in increased NODSNs of 367, 478, 500, 500, and 500 nodes, respectively.

Table 4. NODSN analysis of the IMD-EACBR technique compared to other models under various numbers of rounds.

No. of Dead Sensor Nodes						
No. of Rounds	**IMD-EACBR**	**SFO Alg.**	**GWO Alg.**	**Genetic Alg.**	**ALO Alg.**	**PSO Alg.**
2000	32	56	96	127	205	222
2250	49	92	178	240	295	346
2500	61	108	295	321	368	446
2750	115	188	324	374	415	467
3000	163	275	430	475	481	492
3250	185	324	448	490	495	498
3500	215	367	478	500	500	500
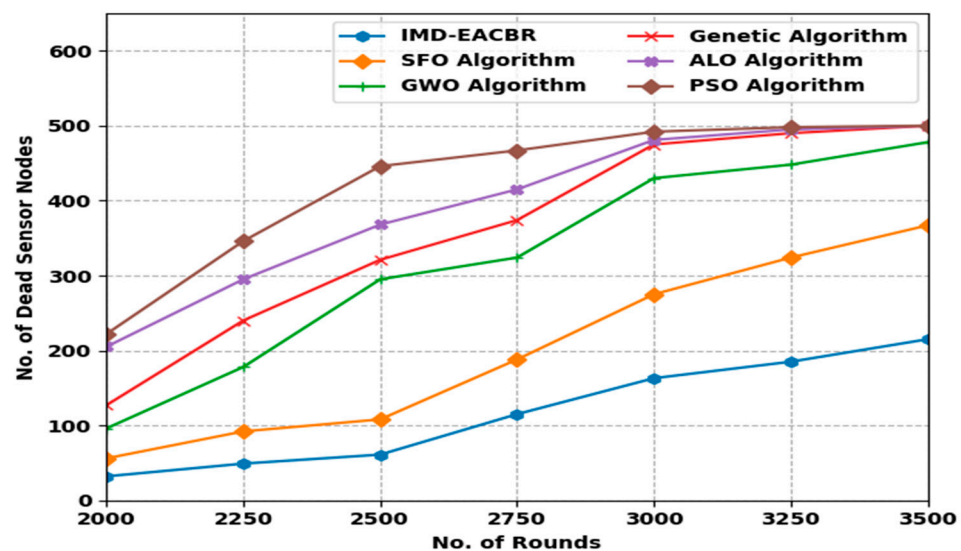
Figure 5. NODSN analysis of the IMD-EACBR technique under various numbers of rounds.

An ephemeral comparative inspection of the IMD-EACBR prototype compared to current algorithms in terms of energy consumption (ECM) is provided in Table 5 and Figure 6. The consequences were that the IMD-EACBR approach outperformed, resulting in effectual outcomes with minimal values of NODSNs. For instance, with 100 SN, the IMD-EACBR approach provided decreased NODSNs of 0.047 mJ, whereas the SFO, GWO, GA, ALO, and PSO models resulted in increased NODSNs of 0.078 mJ, 0.113 mJ, 0.153 mJ, 0.203 mJ, and 0.246 mJ, respectively.

Table 5. ECM analysis of the IMD-EACBR technique compared to other models under different densities of SNs.

| Energy Consumption (mJ)						
Density of Sensor Nodes	**IMD-EACBR**	**SFO Alg.**	**GWO Alg.**	**Genetic Alg.**	**ALO Alg.**	**PSO Alg.**
100	0.047	0.078	0.113	0.153	0.203	0.246
150	0.106	0.149	0.186	0.231	0.321	0.368
200	0.125	0.193	0.262	0.323	0.415	0.442
250	0.240	0.271	0.349	0.431	0.502	0.568
300	0.288	0.337	0.429	0.523	0.563	0.657
350	0.401	0.417	0.580	0.573	0.625	0.686
400	0.417	0.476	0.596	0.658	0.714	0.736
450	0.495	0.509	0.622	0.705	0.773	0.782
500	0.524	0.561	0.625	0.754	0.818	0.846
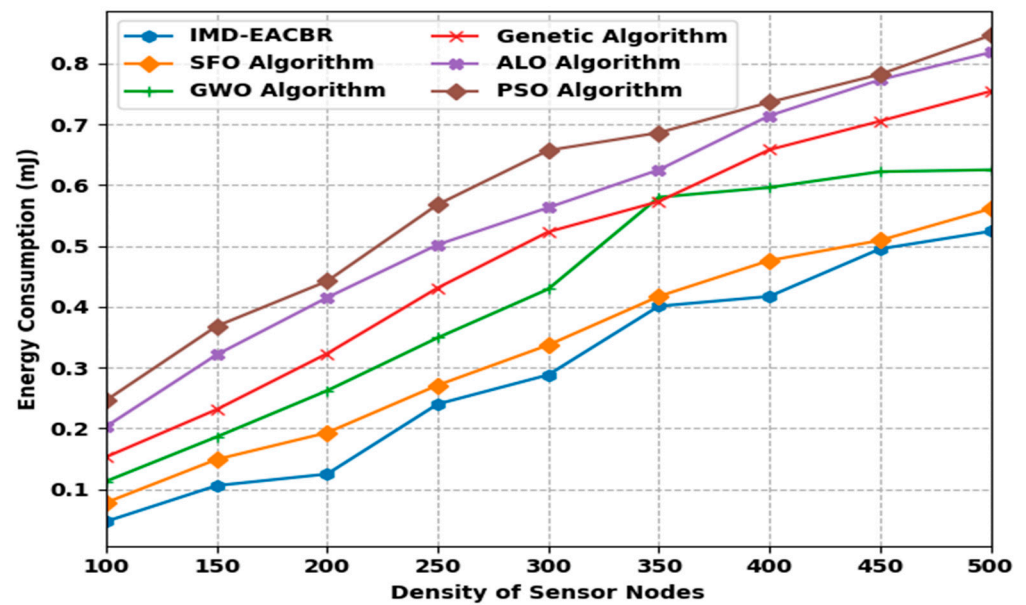
Figure 6. ECM analysis of the IMD-EACBR technique under various densities of SNs.

Table 6 and Figure 7 illustrate a brief throughput (THPT) examination of the IMD-EACBR approach compared to other approaches. The results indicate that the IMD-EACBR methodology demonstrates supreme THPT under all SNs. For example, with 100 SNs, the IMD-EACBR model achieved a higher THPT of 0.975 Mbps, whereas the SFO, GWO, GA, ALO, and PSO techniques achieved lower THPTs of 0.934 Mbps, 0.891 Mbps, 0.861 Mbps, 0.804 Mbps, and 0.704 Mbps, respectively. Eventually, with 500 SNs, the IMD-EACBR approach reached a superior THPT of 0.902 Mbps, while the SFO, GWO, GA, ALO, and PSO techniques resulted in lower THPTs of 0.819 Mbps, 0.728 Mbps, 0.632 Mbps, 0.565 Mbps, and 0.522 Mbps, respectively.

Table 6. Throughput analysis of the IMD-EACBR technique compared to other approaches under different densities of SNs.

	Throughput (Mbps)					
Density of Sensor Nodes	IMD-EACBR	SFO Alg.	GWO Alg.	Genetic Alg.	ALO Alg.	PSO Alg.
100	0.975	0.934	0.891	0.861	0.804	0.704
150	0.967	0.930	0.877	0.805	0.788	0.677
200	0.958	0.916	0.855	0.781	0.762	0.658
250	0.955	0.895	0.838	0.771	0.728	0.636
300	0.945	0.903	0.801	0.745	0.691	0.616
350	0.945	0.878	0.776	0.707	0.656	0.573
400	0.929	0.844	0.776	0.692	0.619	0.569
450	0.913	0.830	0.738	0.667	0.594	0.548
500	0.902	0.819	0.728	0.632	0.565	0.522

Table 7 and Figure 8 depict a brief packet delivery ratio (PDR) analysis of the IMD-EACBR approach compared to existing algorithms. The results indicate that the IMD-EACBR model achieved the greatest PDR under all SNs. For example, with 100 SNs, the IMD-EACBR model reached a PDR of 98.83%, whereas the SFO, GWO, GA, ALO, and PSO systems obtained lower PDRs of 98.40%, 96.47%, 95.65%, 94.37%, and 93.79%, respectively [20,23–27]. Moreover, with 500 SNs, the IMD-EACBR model reached an ultimate PDR of 96.56%, whereas the SFO, GWO, GA, ALO, and PSO methodologies resulted in reduced PDRs of 95.20%, 94.66%, 93.47%, 92.30%, and 91.37%, respectively.
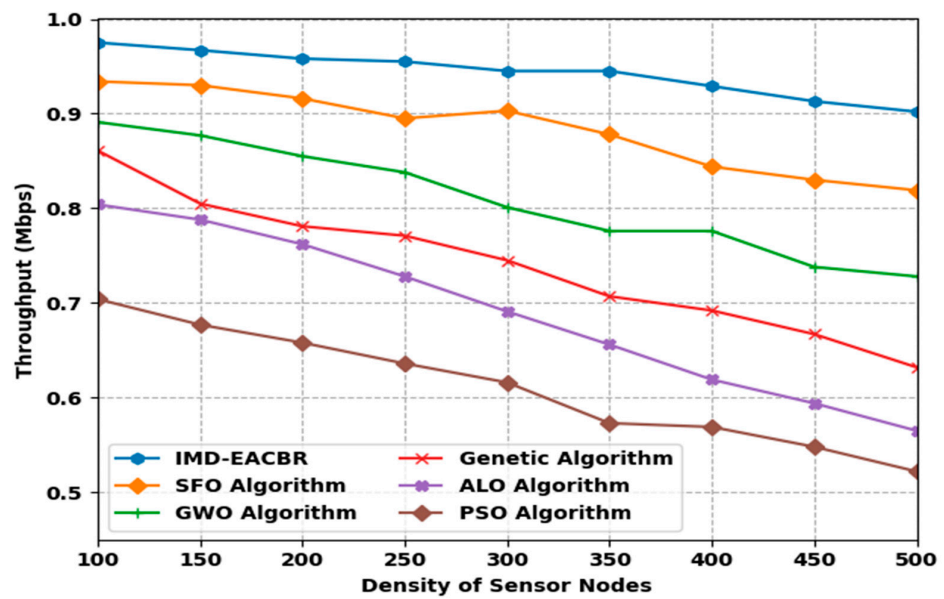
Figure 7. Throughput analysis of the IMD-EACBR technique under different densities of SNs.

Table 7. PDR analysis of the IMD-EACBR technique compared to other approaches under different densities of SNs.

	Packet Delivery Ratio (%)					
Density of Sensor Nodes	IMD-EACBR	SFO Alg.	GWO Alg.	Genetic Alg.	ALO Alg.	PSO Alg.
100	98.83	98.40	96.47	95.65	94.37	93.79
150	98.46	97.90	96.47	95.54	94.07	93.16
200	98.46	97.64	96.43	95.35	93.73	92.82
250	98.25	97.68	96.34	95.13	93.53	92.52
300	98.03	97.40	96.10	94.81	93.29	92.34
350	97.62	96.58	95.85	94.50	92.88	91.97
400	97.19	96.60	95.39	94.35	92.71	91.72
450	96.97	96.15	95.00	93.94	92.52	91.48
500	96.56	95.20	94.66	93.47	92.30	91.37
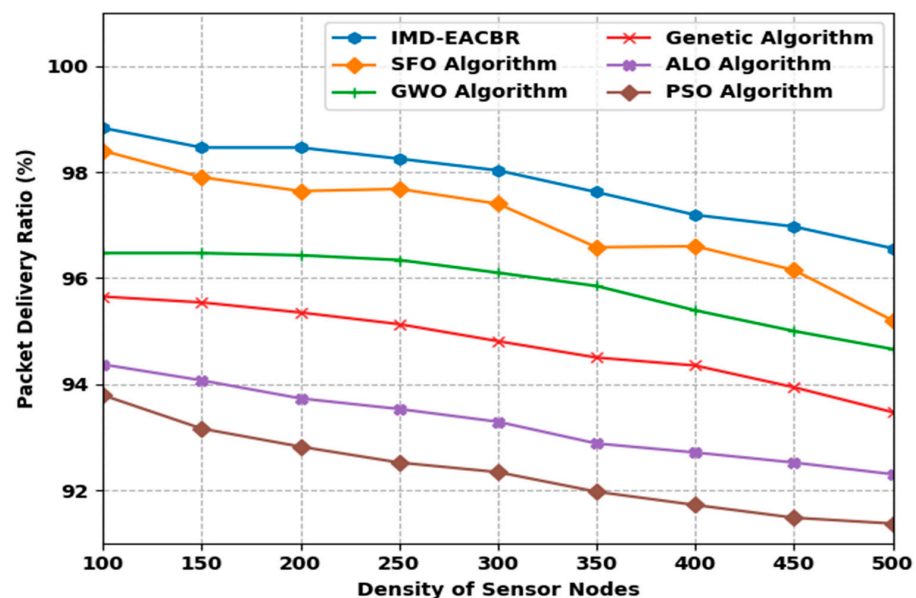
Figure 8. PDR analysis of the IMD-EACBR technique under different densities of SNs.

Finally, a cost function examination of the IMD-EACBR model compared to other optimization techniques is summarised in Figure 9. The results indicate that the GA performed poorly with increased cost function values. The other algorithms, except for the GWO and the IMD-EACBR model, exhibited similar cost function values. Although the GWO algorithm achieved a reasonable outcome, the IMD-EACBR model displayed superior performance. The aforementioned tables and figures report the superiority of the IMD-EACBR approach over all other methods in IoT-assisted WSNs.
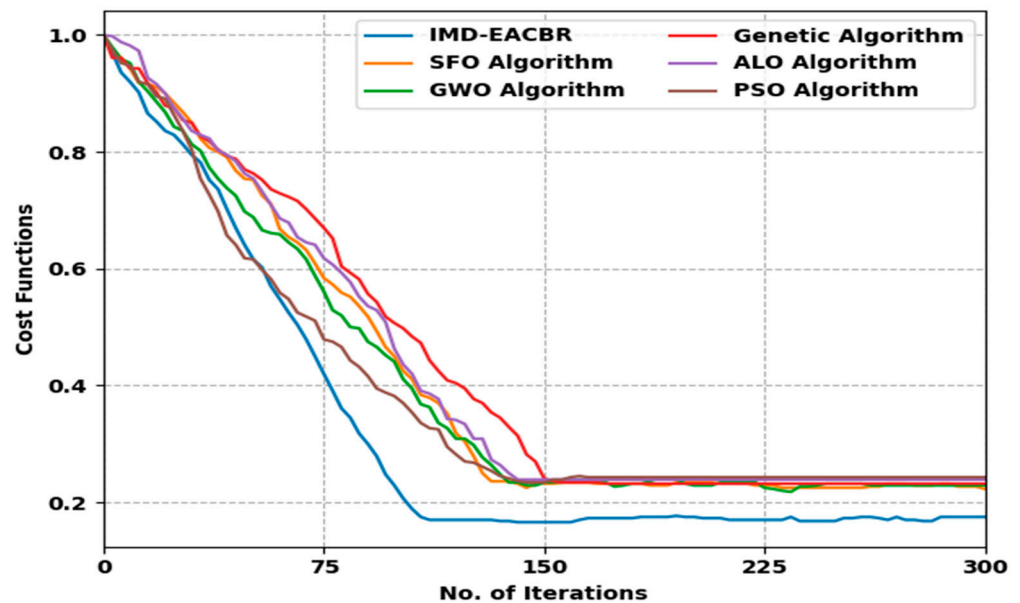
Figure 9. Cost function analysis of the IMD-EACBR technique compared to other methodologies.

5. Conclusions

In this study, a new IMD-EACBR procedure has been designed to maximise the energy efficiency and lifetime of WSNs. At the primary level, the IoT nodes in the network are randomly placed and communicate with one another via information collection processes. Then, the presented IMD-EACBR technique primarily selects CHs and organises clusters using the IAOAC technique. Following this, the optimal selection of routes takes place using the TLBO-MHR technique. Once the optimal routes are identified, the CHs use optimal routes to transmit data to the BS. The recommended protocol makes use of an energy-saving method, in which optimum CHs are chosen on the basis of an improved search equation and an effective fitness function, as opposed to relying on a conventional search procedure. These processes make the protocol more effective. In order to demonstrate that the suggested protocol is valid across a range of presentation criteria, we compared its performance to that of other well-known cluster-based conventions. The design of IAOAC and TLBO-MHR techniques with multiple input parameters helps to achieve maximum network efficiency. The performance of the IMD-EACBR model has been examined in several aspects. The outcomes of the simulation experiments demonstrated the effectiveness of the enhancements of the IMD-EACBR technique over existing approaches. Among the technical limitations of the IMD-EACBR approach is the requirement for parameter tweaking. In the future, the energy efficiency of the IMD-EACBR technique may be further enhanced by data aggregation and sleep scheduling schemes.

References

1. Arjunan, S.; Pothula, S.; Ponnurangam, D. F5N-based unequal clustering protocol (F5NUCP) for wireless sensor networks. *Int. J. Commun. Syst.* **2018**, *31*, e3811. [CrossRef]
2. Rezaeipanah, A.; Amiri, P.; Nazari, H.; Mojarad, M.; Parvin, H. An energy-aware hybrid approach for wireless sensor networks using re-clustering-based multi-hop routing. *Wirel. Pers. Commun.* **2021**, *120*, 3293–3314. [CrossRef]
3. Berlin, M.A.; Tripathi, S.; Devi, V.B.; Bhardwaj, I.; Arulkumar, N. IoT-based traffic prediction and traffic signal control system for smart city. *Soft Comput.* **2021**, *25*, 12241–12248.
4. Norouzi Shad, M.; Maadani, M.; Nesari Moghadam, M. GAPSO-SVM: An IDSS-based energy-aware clustering routing algorithm for IoT perception layer. *Wirel. Pers. Commun.* **2021**, 1–20. [CrossRef]
5. Satpathy, S.; Prakash, M.; Debbarma, S.; Sengupta, A.S.; Bhattacaryya, B.K. Design a FPGA, fuzzy based, insolent method for prediction of multi-diseases in rural area. *J. Intell. Fuzzy Syst.* **2019**, *37*, 7039–7046. [CrossRef]
6. Famila, S.; Jawahar, A.; Sariga, A.; Shankar, K. Improved artificial bee colony optimization based clustering algorithm for SMART sensor environments. *Peer—Peer Netw. Appl.* **2020**, *13*, 1071–1079. [CrossRef]
7. Kavitha, A.; Velusamy, R.L. Simulated annealing and genetic algorithm-based hybrid approach for energy-aware clustered routing in large-range multi-sink wireless sensor networks. *Int. J. Ad Hoc Ubiquitous Comput.* **2020**, *35*, 96–116. [CrossRef]
8. Subbulakshmi, P.; Prakash, M. Mitigating eavesdropping by using fuzzy based MDPOP-Q learning approach and multilevel Stackelberg game theoretic approach in wireless CRN. *Cogn. Syst. Res.* **2018**, *52*, 853–861. [CrossRef]
9. Rajaram, P.V.; Prakash, M. Intelligent deep learning based bidirectional long short term memory model for automated reply of e-mail client prototype. *Pattern Recognit. Lett.* **2021**, *152*, 340–347.
10. Ramalingam, C.; Mohan, P. Addressing semantics standards for cloud portability and interoperability in multi cloud environment. *Symmetry* **2021**, *13*, 317. [CrossRef]
11. Neelakandan, S.; Arun, A.; Bhukya, R.R.; Hardas, B.M.; Kumar, T.; Ashok, M. An Automated Word Embedding with Parameter Tuned Model for Web Crawling. *Intell. Autom. Soft Comput.* **2022**, *32*, 1617–1632. [CrossRef]
12. Mohan, P.; Subramani, N.; Alotaibi, Y.; Alghamdi, S.; Khalaf, O.I.; Ulaganathan, S. Improved metaheuristics-based clustering with multihop routing protocol for underwater wireless sensor networks. *Sensors* **2022**, *22*, 1618. [CrossRef] [PubMed]
13. Anuradha, D.; Subramani, N.; Khalaf, O.I.; Alotaibi, Y.; Alghamdi, S.; Rajagopal, M. Chaotic Search-and-Rescue-Optimization-Based Multi-Hop Data Transmission Protocol for Underwater Wireless Sensor Networks. *Sensors* **2022**, *22*, 2867. [CrossRef]
14. Singh, H.; Ramya, D.; Saravanakumar, R.; Sateesh, N.; Anand, R.; Singh, S.; Neelakandan, S. Artificial intelligence based quality of transmission predictive model for cognitive optical networks. *Optik* **2022**, *257*, 168789. [CrossRef]
15. Subramani, N.; Mohan, P.; Alotaibi, Y.; Alghamdi, S.; Khalaf, O.I. An Efficient Metaheuristic-Based Clustering with Routing Protocol for Underwater Wireless Sensor Networks. *Sensors* **2022**, *22*, 415. [CrossRef] [PubMed]
16. Subahi, A.F.; Alotaibi, Y.; Khalaf, O.I.; Ajesh, F. Packet Drop Battling Mechanism for Energy Aware Detection inWireless Networks. CMC-Computers. *Mater. Contin.* **2020**, *66*, 2077–2086.
17. Palanisamy, S.; Thangaraju, B.; Khalaf, O.I.; Alotaibi, Y.; Alghamdi, S.; Alassery, F. A Novel Approach of Design and Analysis of a Hexagonal Fractal Antenna Array (HFAA) for Next-Generation Wireless Communication. *Energies* **2021**, *14*, 6204. [CrossRef]
18. Pandey, O.J.; Yuvaraj, T.; Paul, J.K.; Nguyen, H.H.; Gundepudi, K.; Shukla, M.K. Improving Energy Efficiency and QoS of LPWANs for IoT Using Q-Learning Based Data Routing. *IEEE Trans. Cogn. Commun. Netw.* **2021**, *8*, 365–379. [CrossRef]
19. Yan, X.; Huang, C.; Gan, J.; Wu, X. Game Theory-Based Energy-Efficient Clustering Algorithm for Wireless Sensor Networks. *Sensors* **2022**, *22*, 478. [CrossRef]
20. Raghavendra, S.; Harshavardhan, A.; Neelakandan, S.; Partheepan, R.; Walia, R.; Rao, V.C.S. Multilayer Stacked Probabilistic Belief Network-Based Brain Tumor Segmentation and Classification. *Int. J. Found. Comput. Sci.* **2022**, 1–24. [CrossRef]

21. Srilakshmi, U.; Veeraiah, N.; Alotaibi, Y.; Alghamdi, S.; Khalaf, O.I.; Subbayamma, B.V. An Improved Hybrid Secure Multipath Routing Protocol for MANET. *IEEE Access* **2021**, *9*, 163043–163053. [CrossRef]
22. Jha, N.; Prashar, D.; Khalaf, O.I.; Alotaibi, Y.; Alsufyani, A.; Alghamdi, S. Blockchain Based Crop Insurance: A Decentralized Insurance System for Modernization of Indian Farmers. *Sustainability* **2021**, *13*, 8921. [CrossRef]
23. Sridevi, M.; Saravanan, C. Deep Learning Approaches for Cyberbullying Detection and Classification on Social Media. *Comput. Intell. Neurosci.* **2022**, *2022*, 2163458. [CrossRef]
24. Sundas, A.; Badotra, S.; Alotaibi, Y.; Alghamdi, S.; Khalaf, O.I. Modified bat algorithm for optimal vm's in cloud computing. *Comput. Mater. Contin.* **2022**, *72*, 2877–2894. [CrossRef]
25. Sennan, S.; Kirubasri; Alotaibi, Y.; Pandey, D.; Alghamdi, S. EACR-LEACH: Energy-aware cluster-based routing protocol for WSN based IoT. *Comput. Mater. Contin.* **2022**, *72*, 2159–2174.
26. Rawat, S.S.; Alghamdi, S.; Kumar, G.; Alotaibi, Y.; Khalaf, O.I.; Verma, L.P. Infrared Small Target Detection Based on Partial Sum Minimization and Total Variation. *Mathematics* **2022**, *10*, 671. [CrossRef]
27. Li, G.; Liu, F.; Sharma, A.; Khalaf, O.I.; Alotaibi, Y.; Alsufyani, A.; Alghamdi, S. Research on the natural language recognition method based on cluster analysis using neural network. *Math. Probl. Eng.* **2021**, *2021*, 9982305. [CrossRef]
28. Kiran, S.; Neelakandan, S.; Reddy, A.P.; Goyal, S.; Maram, B.; Rao, V.C.S. *Wearable Telemedicine Technology for the Healthcare Industry*; Academic Press: Cambridge, MA, USA, 2022; pp. 153–168. [CrossRef]
29. Jain, D.K.; Tyagi, S.K.K.S.; Neelakandan, S.; Prakash, M.; Natrayan, L. Metaheuristic Optimization-based Resource Allocation Technique for Cybertwin-driven 6G on IoE Environment. *IEEE Trans. Ind. Inform.* **2021**, *18*, 4884–4892. [CrossRef]
30. Venu, D.; Mayuri, A.V.R.; Neelakandan, S.; Murthy, G.L.N.; Arulkumar, N.; Shelke, N. An efficient low complexity compression based optimal homomorphic encryption for secure fiber optic communication. *Optik* **2022**, *252*, 168545. [CrossRef]
31. Fathy, A.; Alharbi, A.G.; Alshammari, S.; Hasanien, H.M. Archimedes optimization algorithm based maximum power point tracker for wind energy generation system. *Ain Shams Eng. J.* **2022**, *13*, 101548. [CrossRef]
32. Hemavathi; Akhila, S.R.; Alotaibi, Y.; Khalaf, O.I.; Alghamdi, S. Authentication and Resource Allocation Strategies during Handoff for 5G IoVs Using Deep Learning. *Energies* **2022**, *15*, 2006. [CrossRef]
33. Srilakshmi, U.; Alghamdi, S.; Ankalu, V.V.; Veeraiah, N.; Alotaibi, Y. A secure optimization routing algorithm for mobile ad hoc networks. *IEEE Access* **2022**, *10*, 14260–14269. [CrossRef]
34. Palanisamy, S.; Thangaraju, B.; Khalaf, O.I.; Alotaibi, Y.; Alghamdi, S. Design and Synthesis of Multi-Mode Bandpass Filter for Wireless Applications. *Electronics* **2021**, *10*, 2853. [CrossRef]
35. Sharma, S.; Chakraborty, S.; Saha, A.K.; Nama, S.; Sahoo, S.K. mLBOA: A Modified Butterfly Optimization Algorithm with Lagrange Interpolation for Global Optimization. *J. Bionic Eng.* **2022**, 1–16. [CrossRef]
36. Asha, P.; Natrayan, L.; Geetha, B.T.; Beulah, J.R.; Sumathy, R.; Varalakshmi, G.; Neelakandan, S. IoT enabled environmental toxicology for air pollution monitoring using AI techniques. *Environ. Res.* **2022**, *205*, 112574. [CrossRef] [PubMed]
37. Rao, R.V.; Savsani, V.J.; Vakharia, D.P. Teaching–learning-based optimization: A novel method for constrained mechanical design optimization problems. *Comput. Aided Des.* **2011**, *43*, 303–315. [CrossRef]
38. Perumal, S.K.; Kallimani, J.S.; Ulaganathan, S.; Bhargava, S.; Meckanizi, S. Controlling energy aware clustering and multihop routing protocol for IoT assisted wireless sensor networks. *Concurr. Comput. Pr. Exper.* **2022**, e7106. [CrossRef]
39. Prakash, M.; Ravichandran, T. An efficient resource selection and binding model for job scheduling in grid. *Eur. J. Sci. Res.* **2012**, *81*, 450–458.
40. Mohan, P.; Thangavel, R. Resource selection in grid environment based on trust evaluation using feedback and performance. *Am. J. Appl. Sci.* **2013**, *10*, 924. [CrossRef]
41. Veeraiah, N.; Khalaf, O.I.; Prasad, C.V.P.R.; Alotaibi, Y.; Alsufyani, A.; Alghamdi, S.A.; Alsufyani, N. Trust aware secure energy efficient hybrid protocol for manet. *IEEE Access* **2021**, *9*, 120996–121005. [CrossRef]
42. Alotaibi, Y. A New Secured E-Government Efficiency Model for Sustainable Services Provision. *J. Inf. Secur. Cybercrimes Res.* **2020**, *3*, 75–96. [CrossRef]
43. Prakash, M.; Sayeed, R.F.; Princey, S.; Priyanka, S. Deployment of MultiCloud Environment with Avoidance of DDOS Attack and Secured Data Privacy. *Int. J. Appl. Eng. Res.* **2015**, *10*, 8121–8124.
44. Ramalingam, C.; Mohan, P. An efficient applications cloud interoperability framework using I-Anfis. *Symmetry* **2013**, *13*, 268. [CrossRef]
45. Mohan, P.; Sundaram, M.; Satpathy, S.; Das, S. An efficient technique for cloud storage using secured de-duplication algorithm. *J. Intell. Fuzzy Syst.* **2021**, *41*, 2969–2980. [CrossRef]
46. Ambeth Kumar, V.D.; Malathi, S.; Kumar, A.; Veluvolu, K.C. Active Volume Control in Smart Phones Based on User Activity and Ambient Noise. *Sensors* **2020**, *20*, 4117. [CrossRef] [PubMed]
47. Alotaibi, Y. A New Meta-Heuristics Data Clustering Algorithm Based on Tabu Search and Adaptive Search Memory. *Symmetry* **2022**, *14*, 623. [CrossRef]
48. Anand, J.G. Trust based optimal routing in MANET's. In Proceedings of the 2011 International Conference on Emerging Trends in Electrical and Computer Technology, Nagercoil, India, 23–24 March 2011; pp. 1150–1156. [CrossRef]
49. Kamalraj, R.; Neelakandan, S.; Kumar, M.R.; Rao, V.C.S.; Anand, R.; Singh, H. Interpretable filter based convolutional neural network (IF-CNN) for glucose prediction and classification using PD-SS algorithm. *Measurement* **2021**, *183*, 109804. [CrossRef]

50. Kavitha, T.; Mathai, P.P.; Karthikeyan, C.; Ashok, M.; Kohar, R.; Avanija, J.; Neelakandan, S. Deep Learning Based Capsule Neural Network Model for Breast Cancer Diagnosis Using Mammogram Images. *Interdiscip. Sci. Comput. Life Sci.* **2021**, *14*, 113–129. [CrossRef]

51. Cyril, C.P.D.; Beulah, J.R.; Subramani, N.; Mohan, P.; Harshavardhan, A.; Sivabalaselvamani, D. An automated learning model for sentiment analysis and data classification of Twitter data using balanced CA-SVM. *Concurr. Eng. Res. Appl.* **2021**, *29*, 386–395. [CrossRef]

52. Reshma, G.; Al-Atroshi, C.; Nassa, V.K.; Geetha, B.; Sunitha, G.; Galety, M.G.; Neelakandan, S. Deep Learning-Based Skin Lesion Diagnosis Model Using Dermoscopic Images. *Intell. Autom. Soft Comput.* **2022**, *31*, 621–634. [CrossRef]

53. Kannan, K.S.; Suma, K.G. A Secured Healthcare Medical System Using Blockchain Technology. In *ICCCE 2021*; Lecture Notes in Electrical Engineering; Kumar, A., Mozar, S., Eds.; Springer: Singapore, 2022; Volume 828. [CrossRef]

54. Sunitha, G.; Geetha, K.; Neelakandan, S.; Pundir, A.K.S.; Hemalatha, S.; Kumar, V. Intelligent deep learning based ethnicity recognition and classification using facial images. *Image Vis. Comput.* **2022**, *121*, 104404. [CrossRef]

55. Parthiban, S.; Harshavardhan, A.; Neelakandan, S.; Prashanthi, V.; Alolo, A.-R.A.A.; Velmurugan, S. Chaotic Salp Swarm Optimization-Based Energy-Aware VMP Technique for Cloud Data Centers. *Comput. Intell. Neurosci.* **2022**, *2022*, 4343476. [CrossRef] [PubMed]

56. Bharany, S.; Sharma, S.; Badotra, S.; Khalaf, O.I.; Alotaibi, Y.; Alghamdi, S.; Alassery, F. Energy-Efficient Clustering Scheme for Flying Ad-Hoc Networks Using an Optimized LEACH Protocol. *Energies* **2021**, *14*, 6016. [CrossRef]

57. Harshavardhan, A.; Boyapati, P.; Neelakandan, S.; Akeji, A.A.A.-R.; Pundir, A.K.S.; Walia, R. LSGDM with Biogeography-Based Optimization (BBO) Model for Healthcare Applications. *J. Healthc. Eng.* **2022**, *2022*, 2170839. [CrossRef]

58. Alotaibi, Y. Automated Business Process Modelling for Analyzing Sustainable System Requirements Engineering. In Proceedings of the 2020 6th International Conference on Information Management, London, UK, 27–29 March 2020; pp. 157–161.

59. Suryanarayana, G.; Chandran, K.; Khalaf, O.I.; Alotaibi, Y.; Alsufyani, A.; Alghamdi, S.A. Accurate Magnetic Resonance Image Super-Resolution Using Deep Networks and Gaussian Filtering in the Stationary Wavelet Domain. *IEEE Access* **2021**, *9*, 71406–71417. [CrossRef]

60. Rout, R.; Parida, P.; Alotaibi, Y.; Alghamdi, S.; Khalaf, O.I. Skin Lesion Extraction Using Multiscale Morphological Local Variance Reconstruction BasedWatershed Transform and Fast Fuzzy C-Means Clustering. *Symmetry* **2021**, *13*, 2085. [CrossRef]

61. Geetha, B.; Kumar, P.S.; Bama, B.S.; Neelakandan, S.; Dutta, C.; Babu, D.V. Green energy aware and cluster-based communication for future load prediction in IoT. *Sustain. Energy Technol. Assess.* **2022**, *52*, 102244–102256. [CrossRef]

62. Rayen, S.J.; Arunajsmine, J. Social Media Networks Owing To Disruptions For Effective Learning. *Procedia Comput. Sci.* **2020**, *172*, 145–151. [CrossRef]

63. Divyabharathi, S. Large scale optimization to minimize network traffic using MapReduce in big data applications. In Proceedings of the International Conference on Computation of Power, Energy Information and Communication (ICCPEIC), Melmaruvathur, India, 20–21 April 2016; pp. 193–199. [CrossRef]

64. Neelakandan, S.; Rene Beulah, J.; Prathiba, L.; Murthy GL, N.; Irudaya Raj, E.F.; Arulkumar, N. Blockchain with deep learning-enabled secure healthcare data transmission and diagnostic model. *Int. J. Modeling Simul. Sci. Comput.* **2022**, 2241006. [CrossRef]

65. Neelakandan, S.; Prakash, M.; Bhargava, S.; Mohan, K.; Robert, N.R.; Upadhye, S. Optimal Stacked Sparse Autoencoder Based Traffic Flow Prediction in Intelligent Transportation Systems. In *Studies in Systems, Decision and Control*; Springer: Cham, Switzerland, 2022; Volume 412. [CrossRef]

66. Paulraj, D. A gradient boosted decision tree-based sentiment classification of twitter data. *Int. J. Wavelets Multiresolution Inf. Process.* **2020**, *8*, 205027. [CrossRef]

67. Paulraj, D. An Automated Exploring and Learning Model for Data Prediction Using Balanced CA-SVM. *J. Ambient. Intell. Humaniz. Comput.* **2020**, *12*, 4979–4990. [CrossRef]

68. Rajendran, S.; Khalaf, O.I.; Alotaibi, Y.; Alghamdi, S. MapReduce-based big data classification model using feature subset selection and hyperparameter tuned deep belief network. *Sci. Rep.* **2021**, *11*, 24138. [CrossRef] [PubMed]

69. Kavitha, M.; Babu, B.S.; Sumathy, B.; Jackulin, T.; Ramkumar, N.; Manimaran, A.; Walia, R.; Neelakandan, S. Convolutional neural networks-based video reconstruction and computation in digital twins. *Intell. Autom. Soft Comput.* **2022**, *34*, 1571–1586. [CrossRef]

70. Pandey, O.J.; Hegde, R.M. Low-Latency and Energy-Balanced Data Transmission Over Cognitive Small World WSN. *IEEE Trans. Veh. Technol.* **2018**, *67*, 7719–7733. [CrossRef]